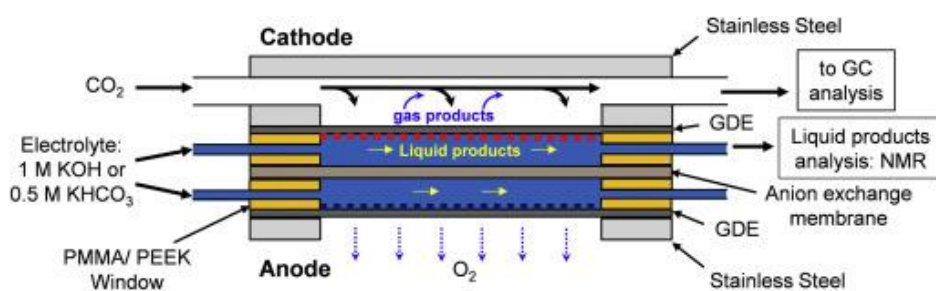


## Supporting information

### High efficiency electrochemical reduction of CO<sub>2</sub> beyond two-electron transfer pathway on grain boundary rich ultra-small SnO<sub>2</sub> nanoparticles

Chenglu Liang,<sup>†ab</sup> Byoungsu Kim,<sup>†cd</sup> Shize Yang,<sup>†e</sup> Yang Liu,<sup>ab</sup> Cristiano Francisco Woellner,<sup>b</sup> Zhengyuan Li,<sup>b</sup> Robert Vajtai,<sup>b</sup> Wei Yang,<sup>\*a</sup> Jingjie Wu,<sup>\*f</sup> Paul J.A. Kenis<sup>\*cd</sup> and Pulickel M. Ajayan<sup>b\*</sup>



**Fig. S1.** Schematic of flow cell for CO<sub>2</sub> reduction. (Ref. One-step electrosynthesis of ethylene and ethanol from CO<sub>2</sub> in an alkaline electrolyzer)<sup>[1]</sup>

An electrochemical flow cell reported previously is used as the CO<sub>2</sub> electrolyzer. A schematic of the flow cell used in this study is shown in Fig. S1. In this work, an anion exchange membrane (Fumatech®) is inserted between the catholyte and anolyte chamber to prevent the liquid products from diffusing to the anode where they may get oxidized. Stainless steel plates (5.5 " 2.5 cm) serve as current collectors to hold the flow cell together via a squeeze-action toggle plier clamp (McMaster Carr 5062A63) and provide electrical contact between the GDE and an external potentiostat (Autolab, PGSTAT-30, EcoChemie). Two 1.5-mm thick polyether ether ketone (PEEK) spacers with a precisely machined 0.5-cm wide by 2.0-cm long window provide the catholyte and anolyte flow fields, respectively. The cathode current collector has a precisely machined 0.5-cm wide by 2.0-cm long window with 0.5 cm depth behind the GDE to allow for the flow of gases. The anode is open to air, allowing oxygen to escape.

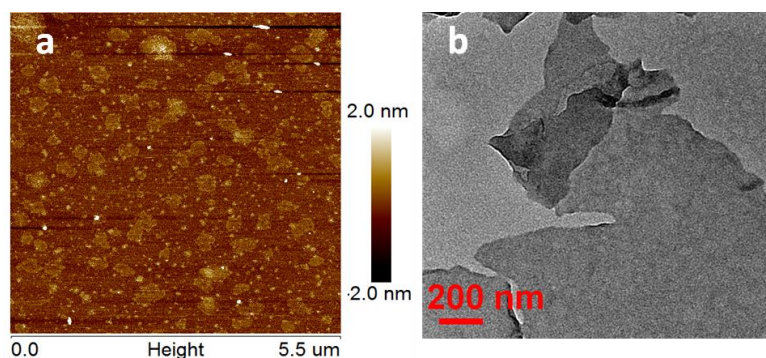


**Fig. S2.** (a)AFM Picture of SnS<sub>2</sub> Sheets, (b) TEM Picture of SnS<sub>2</sub> Sheets.

The AFM picture of SnS<sub>2</sub> sheets showed the morphology of typical exfoliated 2D materials. The thickness of SnS<sub>2</sub> sheets was in the range of 0.8~1.8nm, indicating the existence of single or few layer SnS<sub>2</sub> sheets. The TEM picture of SnS<sub>2</sub> sheets further confirmed the layer structure.

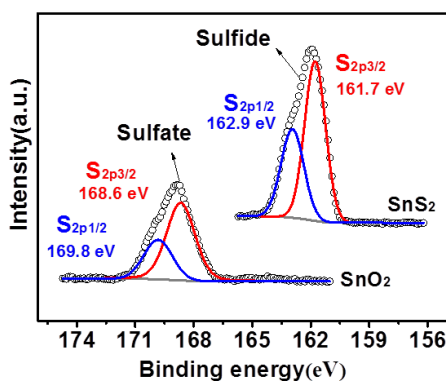


**Fig. S3.** S<sub>2p</sub> XPS spectra of SnS<sub>2</sub> sheets and SnO<sub>2</sub> nanoparticles

The S<sub>2p</sub> XPS spectra shown in Fig. S3 can provide further evidence for the complete transformation from SnS<sub>2</sub> to SnO<sub>2</sub>. The S<sub>2p</sub> XPS spectrum of original SnS<sub>2</sub> nanosheets can be deconvoluted into two peaks at 162.9 eV and 161.7 eV, corresponding to the 2P<sub>1/2</sub> and 2P<sub>3/2</sub> binding energies of SnS<sub>2</sub>. When oxidized to SnO<sub>2</sub> nanoparticles, the sulfide was transformed to sulfate chemical structure which shows higher binding energies at 169.8 eV and 168.6 eV for the 2P<sub>1/2</sub> and 2P<sub>3/2</sub> respectively.

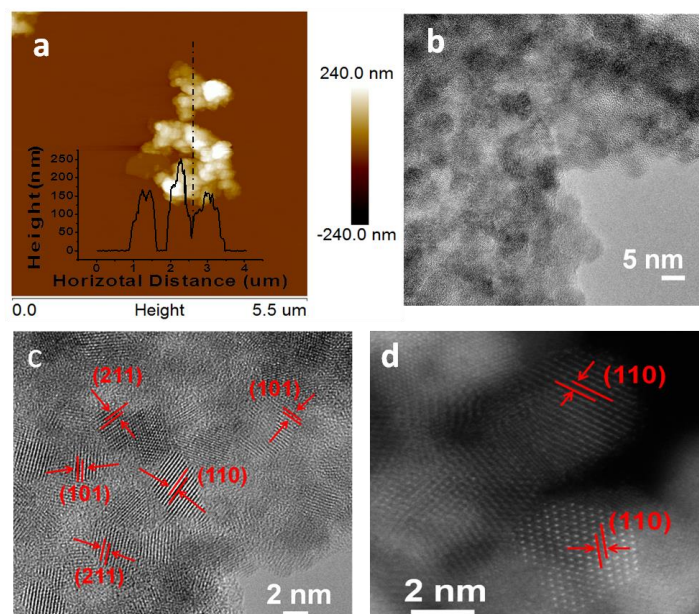


**Fig. S4.** (a) AFM Picture of SnO<sub>2</sub> nanoparticles, (b)(c)(d)TEM Pictures of SnO<sub>2</sub> nanoparticles.

The AFM picture of SnS<sub>2</sub> sheets after hydrothermal reaction (SnO<sub>2</sub> nanoparticles) showed the morphology of aggregated nanoparticles, which was drastically different from the AFM picture of the original SnS<sub>2</sub> sheets. The corresponding TEM pictures showed the detailed and precise morphology of well-defined nanocrystals with uniform size of about 5nm. In the high magnifications of TEM pictures, measured interplanar spacings of 0.335nm, 0.264nm and 0.176nm corresponding to the (110), (101) and (211) of SnO<sub>2</sub> respectively indicated the chemical nature of nanoparticles to be SnO<sub>2</sub>, which was consistent with XRD results.

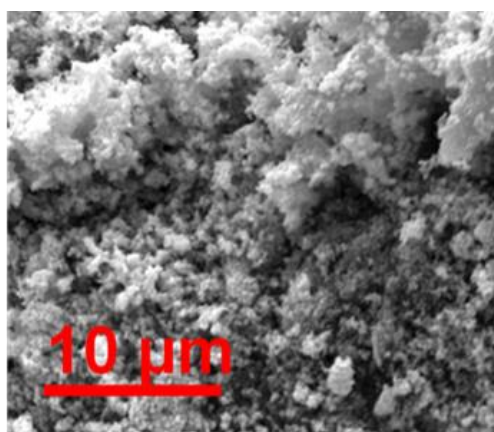


**Fig. S5.** SEM Pictures of bulk SnO<sub>2</sub>(obtained by annealing the bulk SnS<sub>2</sub> at 500°C for 3h in air condition).

The SEM pictures of bulk SnO<sub>2</sub> showed a morphology of aggregated particles with size ranging from 200nm to 500nm. The crystallite size of bulk SnO<sub>2</sub> particles was calculated to be around 28 nm using Debye-Scherrer equation from the XRD result.

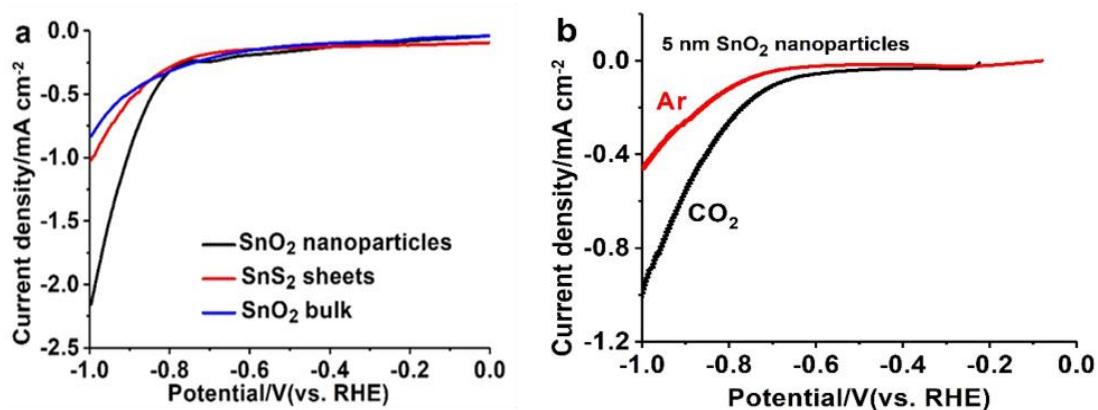


**Fig. S6.** Linear sweep voltammetric curves in the Ar<sub>2</sub>-saturated 1M KOH electrolyte(a) and Ar/CO<sub>2</sub> saturated 0.1 M KHCO<sub>3</sub> (b)

The linear sweep voltammetry (LSV) measurement was implemented in a three-electrode system at a potentiostat (Autolab PGSTAT-30, EcoChemie). The working electrode was a glassy carbon electrode. The platinum gauze and the Ag/AgCl electrode served as counter and the reference electrodes, respectively. In a typical prepared procedure of the working electrode, 3  $\mu$ L of the homogeneous ink, which was prepared by dispersing 5 mg sample and 40  $\mu$ L Nafion solution (5 wt%) in 1 ml water-ethanol solution with volume ratio of 3:1, was loaded onto a glassy carbon electrode with 3 mm diameter. LSV measurement with a scan rate of 20 mV s<sup>-1</sup> was carried out in Ar-saturated 1M KOH (60 ml). As revealed by the LSV results shown in Fig.S6, the SnO<sub>2</sub> nanoparticles exhibited the highest current density among the samples, which was roughly 2 and 3 times larger than that of SnS<sub>2</sub> sheets and SnO<sub>2</sub> bulk, respectively, indicating the higher surface area in SnO<sub>2</sub> nanoparticles. The comparison of LSV in Ar<sub>2</sub> and CO<sub>2</sub> saturated 0.1 M KHCO<sub>3</sub> shows the typical increasing of current density in CO<sub>2</sub> saturated electrolyte, a potential indicator of CO<sub>2</sub> reduction activity on SnO<sub>2</sub> nanoparticles.

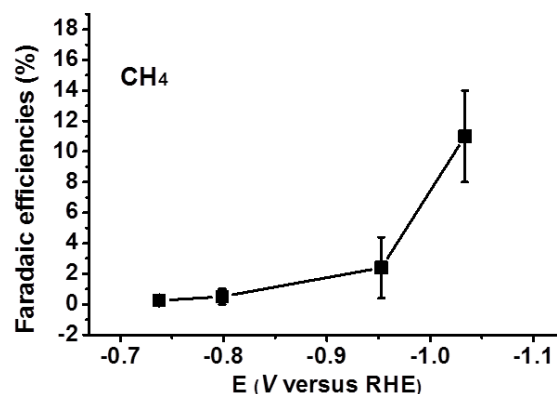


**Fig. S7.** Faradaic efficiencies for CH<sub>4</sub> formation on SnO<sub>2</sub> nanoparticle electrode in 1M KOH electrolyte.

The noticeable average amounts of 2% CH<sub>4</sub> and 11% CH<sub>4</sub> detected at applied potentials of -0.95V and -1.03V respectively, shown Fig. S7 should be emphasized

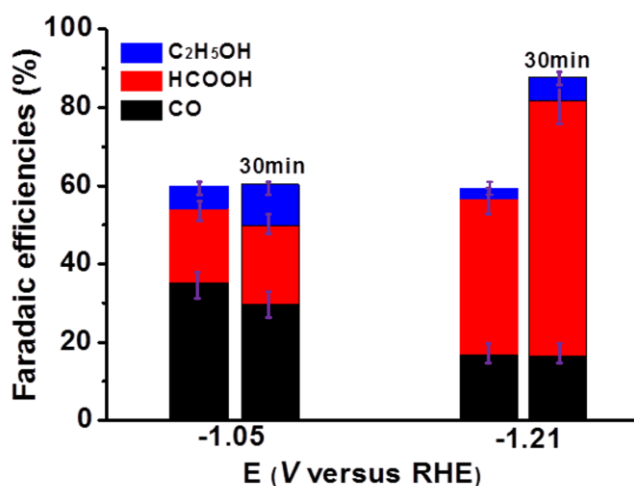


**Fig. S8.** Faradaic efficiencies for CO<sub>2</sub> reduction on SnO<sub>2</sub> nanoparticle electrode tested in 1M KHCO<sub>3</sub> electrolyte before and after 30min electrolysis in the electrolyte, respectively.

It is interesting to find that when the SnO<sub>2</sub> nanoparticle catalyst was tested in the electrolyte of KHCO<sub>3</sub>, C<sub>2</sub>H<sub>5</sub>OH showed a higher selectivity over CH<sub>4</sub>, reaching a FE of 5.8% at -1.05V aside from the main products of CO (FE of 35.3%) and HCOO<sup>-</sup> (FE of 18.8%) as shown in Fig. S8. While the applied potential was more negative(-1.21 V), a higher FE of HCOO<sup>-</sup> (39.6%) was achieved. After the SnO<sub>2</sub> nanoparticle catalyst was under electrolysis for 30 min, the FE of C<sub>2</sub>H<sub>5</sub>OH increased from 5.8% to 10.4% at -1.05V, from 2.5% to 6.0% at -1.21V, possibly due to the component change in the metastable SnO<sub>x</sub>/Sn layer after electrolysis under reduction potentials for 30 min.

## References

- [1] S. Ma, M. Sadakiyo, R. Luo, M. Heima, M. Yamauchi, P.J.A. Kenis, One-step electrosynthesis of ethylene and ethanol from CO<sub>2</sub> in an alkaline electrolyzer, *J. Power Sources*, 301 (2016) 219-228.